

DE LA RECHERCHE À L'INDUSTRIE

cea



[www.cea.fr](http://www.cea.fr)  
[www.ljll.math.upmc.fr](http://www.ljll.math.upmc.fr)

# High-order accurate Lagrange-remap hydrodynamic schemes on staggered Cartesian grids

Gautier DAKIN<sup>1,2</sup>  
Hervé JOURDREN<sup>2</sup>

<sup>1</sup> Université Pierre et Marie Curie,  
LJLL, Paris, France  
<sup>2</sup> CEA, DAM, DIF, F-91297 Arpajon,  
France

February 9, 2016

- 1 Context
- 2 1D-Lagrangian schemes on staggered grids
- 3 1D-Lagrange-Remap Eulerian schemes
- 4 nD Cartesian grids extension *via* high-order accurate directionnal splitting
- 5 Conclusions

Context

## A few among many high-order methods for CFD

- Cell-centered **Godunov-type** schemes
  - Direct Eulerian ENO/WENO finite difference/volume schemes [Shu, 2003],
  - Non-oscillatory central differencing schemes [Nessyahu and Tadmor, 1990]
  - Compact schemes [Nagarajan et al., 2003]
  - GoHy schemes, Cauchy–Kovalevskaya procedure and high-order directionnal splitting in a Lagrange-remap setting on Cartesian grids [Duboc et al., 2010],
- Schemes for unstructured meshes
  - Discontinuous Galerkin (DG) methods [Cockburn et al., 2000],
  - DG spectral element methods [Karniadakis and Sherwin, 2013]
  - DG high-order Riemann solver with the ADER schemes [Titarev and Toro, 2002]

## And for structured staggered grids ?

There are no truly high-order accurate finite volume schemes currently available on **staggered** Cartesian grids .

## Shock capturing schemes on staggered grids

- *Lagrangian* vNR scheme in internal energy : [Richtmyer, 1948] [von Neumann and Richtmyer, 1950]
- Limits of vNR scheme [Trulio and Trigger, 1961]
- $2^{nd}$  order *Eulerian* Lagrange-remap scheme on **staggered Cartesian grids**: KRAKEN [DeBar, 1974] and BBC [Sutcliffe, 1974] hydrocodes, *implicit* 1-iteration fixed point Trulio-Trigger version , *explicit* version [Woodward and Colella, 1984]
- Works for *B-type* staggering (nodal) [Youngs, 2007] and improvement for energy conservation for *C-type* staggering (MAC) [Herbin et al., 2013]
- Beyond  $2^{nd}$  order, there is no truly high-order accurate scheme for the Euler system on staggered Cartesian grids.

## Aim of this work

Building a family of high-order accurate and conservative finite volume schemes on staggered Cartesian grids [Dakin and Jourdain, 2016].

1D-Lagrangian schemes on  
staggered grids

## Variables

- $u$  the material velocity,
- $x$  the position,
- $\rho$  the material density,  $\rho_0$  the initial density,
- $\tau = \frac{1}{\rho}$  the specific volume,
- $e = \epsilon + e_{\text{kin}}$  total, internal and kinetic energy,
- $p$  the pressure,  $q$  the pseudo-viscosity [Richtmyer, 1948, von Neumann and Richtmyer, 1950, Cook and Cabot, 2005],  $\Pi = p + q$ .

## 1D Euler system

$$\begin{cases} \partial_t \rho + \partial_x (\rho u) = 0 \\ \partial_t (\rho u) + \partial_x (\rho u^2 + p) = 0 \\ \partial_t (\rho e) + \partial_x (\rho u e + p u) = 0 \end{cases} \quad (1)$$

## 1D Euler system

$$\left\{ \begin{array}{l} \partial_t \rho + \partial_x (\rho u) = 0 \\ \partial_t (\rho u) + \partial_x (\rho u^2 + p) = 0 \\ \partial_t (\rho \epsilon) + \partial_x (\rho u \epsilon) + p \partial_x u = 0 \\ \partial_t (\rho e_{\text{kin}}) + \partial_x (\rho u e_{\text{kin}}) + u \partial_x p = 0 \end{array} \right. \quad (2)$$

## Non conservative terms

We are aiming at solving system (1) but with formulation of system (2).

- For sufficiently smooth problem, there is no special treatments for  $u \partial_x p$  and  $p \partial_x u$  and both systems are equivalent.
- However, when dealing with shocks, there is no sense in writing  $u \partial_x p$  and  $p \partial_x u$ .

So we will introduce a procedure so that for shocks, we are solving system (1).



We make the following change of variables:

$$dx(X, t) = J(X, t)dX + u(X, t)dt$$

which gives the lagrangian system formulated in total energy or in internal and kinetic energies,

## 1D Lagrangian system

$$\left\{ \begin{array}{l} \partial_t (\rho_0 \tau) - \partial_X u = 0 \\ \partial_t (\rho_0 u) + \partial_X p = 0 \\ \partial_t (\rho_0 e) + \partial_X p u = 0 \end{array} \right. \text{rewrites formally} \left\{ \begin{array}{l} \partial_t (\rho_0 \tau) - \partial_X u = 0 \\ \partial_t (\rho_0 u) + \partial_X p = 0 \\ \partial_t (\rho_0 \epsilon) + p \partial_X u = 0 \\ \partial_t (\rho_0 e_{\text{kin}}) + u \partial_X p = 0 \end{array} \right. \quad (3)$$

The closure of the system is realized thanks to the equation of state

$$p = EOS(\tau, \epsilon)$$

## Staggered grids

- A *primal* uniform Cartesian grid  $\{x_{i+\frac{1}{2}}\}$  with  $\Delta X = x_{i+\frac{1}{2}} - x_{i-\frac{1}{2}}$
- A *dual* grid  $\{x_i\}$  with  $x_i = \frac{1}{2}(x_{i+\frac{1}{2}} + x_{i-\frac{1}{2}})$ .

$$\left\{ \begin{array}{l} \bar{\phi}_i^n = \frac{1}{\Delta X} \int_{x_{i-\frac{1}{2}}}^{x_{i+\frac{1}{2}}} \phi(x, t^n) dx, \quad \phi_i^n = \phi(x_i, t^n), \quad \phi \in \{\rho_0, \rho_0 \tau, \rho_0 \epsilon\} \\ \bar{\phi}_{i+\frac{1}{2}}^n = \frac{1}{\Delta X} \int_{x_i}^{x_{i+1}} \phi(x, t^n) dx, \quad \phi_{i+\frac{1}{2}}^n = \phi(x_{i+\frac{1}{2}}, t^n), \quad \phi \in \{\rho_0, \rho_0 u, \rho_0 e_{\text{kin}}\} \end{array} \right.$$

$$d\phi_i = \phi_{i+\frac{1}{2}} - \phi_{i-\frac{1}{2}} \quad \text{and} \quad d\phi_{i+\frac{1}{2}} = \phi_{i+1} - \phi_i. \quad (4)$$

For a grid with  $N$  cells, we have to keep in memory at least  $6N$  variables, whereas for MAC-type it is  $3N$  ([Herbin et al., 2013]).

## Runge-Kutta Finite-Volume (FV) schemes

- Formulated in *internal energy*.
- *Centred* for thermodynamics variables, *staggered* for the mechanical variables, no staggering in time.<sup>a</sup>
- Conservative in mass, momentum and total energy.

---

<sup>a</sup>Trulio-Trigger type: *staggered* in space, *unstaggered* in time

Usual Runge-Kutta notations:

- $\alpha_m$  → time step for the  $m$  subcycle
- $a_{m,l}$  → Butcher's table coefficients
- $\theta_l$  → Reconstruction coefficients

$$\left\{ \begin{array}{l} \overline{\rho_0 \tau}_i^{n+\alpha_m} = \overline{\rho_0 \tau}_i^n + \frac{\Delta t}{\Delta X} \sum_{l=0}^{m-1} a_{m,l} du_i^{n+\alpha_l} \\ \overline{\rho_0 u}_{i+\frac{1}{2}}^{n+\alpha_m} = \overline{\rho_0 u}_{i+\frac{1}{2}}^n - \frac{\Delta t}{\Delta X} \sum_{l=0}^{m-1} a_{m,l} d\Pi_{i+\frac{1}{2}}^{n+\alpha_l} \\ \overline{\rho_0 \epsilon}_i^{n+\alpha_m} = \overline{\rho_0 \epsilon}_i^n - \frac{\Delta t}{\Delta X} \sum_{l=0}^{m-1} a_{m,l} \overline{\Pi \delta u}_i^{n+\alpha_l} \\ x_{i+\frac{1}{2}}^{n+\alpha_m} = x_{i+\frac{1}{2}}^n + \Delta t \sum_{l=0}^{m-1} a_{m,l} u_{i+\frac{1}{2}}^{n+\alpha_l} \\ p_i^{n+\alpha_m} = EOS(\tau_i^{n+\alpha_m}, \epsilon_i^{n+\alpha_m}) \end{array} \right. \quad (5)$$

## Remark

- EOS is called on reconstructed pointwise values thanks to average values.
- Kinetic energy is not updated during the subcycles.

$$\left\{ \begin{array}{l}
 \overline{\rho_0 \tau}_i^{n+1} = \overline{\rho_0 \tau}_i^n + \frac{\Delta t}{\Delta X} \sum_{l=0}^{s-1} \theta_l du_i^{n+\alpha_l} \\
 \overline{\rho_0 u}_{i+\frac{1}{2}}^{n+1} = \overline{\rho_0 u}_{i+\frac{1}{2}}^n - \frac{\Delta t}{\Delta X} \sum_{l=0}^{s-1} \theta_l d\Pi_{i+\frac{1}{2}}^{n+\alpha_l} \\
 \overline{\rho_0 \epsilon}_i^{n,*} = \overline{\rho_0 \epsilon}_i^n - \frac{\Delta t}{\Delta X} \sum_{l=0}^{s-1} \theta_l \overline{\Pi \delta u}_i^{n+\alpha_l} \\
 \overline{\rho_0 e_{\text{kin}}}_{i+\frac{1}{2}}^{n,*} = \overline{\rho_0 e_{\text{kin}}}_{i+\frac{1}{2}}^n - \frac{\Delta t}{\Delta X} \sum_{l=0}^{s-1} \theta_l \overline{u \delta \Pi}_{i+\frac{1}{2}}^{n+\alpha_l} \\
 x_{i+\frac{1}{2}}^{n+1} = x_{i+\frac{1}{2}}^n + \Delta t \sum_{l=0}^{s-1} \theta_l u_{i+\frac{1}{2}}^{n+\alpha_l} \\
 p_i^{n+1} = EOS(\tau_i^{n+1}, \epsilon_i^{n+1})
 \end{array} \right. \quad (6)$$

$$\left\{ \begin{array}{l} \phi_{\xi(i)} = \sum C_k \bar{\phi}_{\xi(i)+k} \\ \bar{\phi}_{\xi(i)} = \sum_k \hat{C}_k \phi_{\xi(i)+k} \\ \phi_{\xi(i)} = \frac{(\rho_0 \phi)_{\xi(i)}}{(\rho_0)_{\xi(i)}} \\ \delta \phi_{\xi(i)} = \sum_{k \geq 0} d_k \left( \phi_{\xi(i)+k+\frac{1}{2}} - \phi_{\xi(i)-k-\frac{1}{2}} \right) \end{array} \right. \quad \text{with } \xi(i) = \begin{cases} i & \text{on primal grid} \\ i + \frac{1}{2} & \text{on dual grid} \end{cases} \quad (7)$$

## Remark

Coefficients  $C_k$ ,  $\hat{C}_k$  and  $d_k$  are independent of the grid as far as the original grid is Cartesian.

**Table 1 :** Coefficients for the finite volume computation of point-wise values from cell-average ones and *vice versa*.

Order	$C_0$	$C_{\pm 1}$	$C_{\pm 2}$	$C_{\pm 3}$	$\widehat{C}_0$	$\widehat{C}_{\pm 1}$	$\widehat{C}_{\pm 2}$	$\widehat{C}_{\pm 3}$
$2^{nd}$	1	0	0	0	1	0	0	0
$3^{rd}$	$\frac{13}{12}$	$\frac{-1}{24}$	0	0	$\frac{11}{12}$	$\frac{1}{24}$	0	0
$4^{th}$ and $5^{th}$	$\frac{1067}{960}$	$\frac{-29}{480}$	$\frac{3}{640}$	0	$\frac{863}{960}$	$\frac{77}{1440}$	$\frac{-17}{5760}$	0
$6^{th}$ and $7^{th}$	$\frac{30251}{26880}$	$\frac{-7621}{107520}$	$\frac{159}{17920}$	$\frac{-5}{7168}$	$\frac{215641}{241920}$	$\frac{6361}{107520}$	$\frac{-281}{53760}$	$\frac{367}{967680}$

## Remark

Although other reconstructions may be used, centered and symmetric ones are retained here and sufficient for *uniform* Cartesian grids.

**Table 2 :** Coefficients for the  $\delta$  operator and the interpolation of dual grid positions from primal grid ones.

Order	$d_0$	$d_1$	$d_2$	$d_3$	$r_0$	$r_1$	$r_2$	$r_3$
$2^{nd}$	1	0	0	0	$\frac{1}{2}$	0	0	0
$3^{rd}$	$\frac{9}{8}$	$\frac{-1}{24}$	0	0	$\frac{9}{16}$	$\frac{-1}{16}$	0	0
$4^{th}$ and $5^{th}$	$\frac{75}{64}$	$\frac{-25}{384}$	$\frac{3}{640}$	0	$\frac{75}{128}$	$\frac{-25}{256}$	$\frac{3}{256}$	0
$6^{th}$ and $7^{th}$	$\frac{1225}{1024}$	$\frac{-245}{3072}$	$\frac{49}{5120}$	$\frac{-5}{7168}$	$\frac{1225}{2048}$	$\frac{-245}{2048}$	$\frac{49}{2048}$	$\frac{-5}{2048}$

## Remark

The non-conservative terms  $\overline{\psi\delta\phi}$  on RHS of (5) and (6) are computed by:

- 1 Applying the  $\delta$  operator to point-wise values of  $\phi$  using coefficients in Table 2 and last equation of (7).
- 2 Multiplying by point-wise value of  $\psi$ , then reconstructing average values using the right part of Table 1 and second equation of (7).



## Lemma 1

*For all Runge-Kutta sequences, all artificial viscosities, all spatial reconstructions, the schemes (5-7) formulated in internal energy are conservative in mass, momentum. It is also conservative in total energy in the sense that  $E^{n,*} = E^n$  for*

$$E = \sum_i \overline{\rho_0 \epsilon_i} + \sum_i \overline{\rho_0 e_{kin i + \frac{1}{2}}} \quad (8)$$

## Remark

The proof is obvious for mass and momentum and purely algebraic (see next slide) for total energy using summation over the whole space of kinetic and internal energy for wall<sup>a</sup> and periodic boundary conditions.<sup>b</sup>

<sup>a</sup>Ghost-cell values are non-trivial in this case

<sup>b</sup>Definition of total energy on a cell, function of kinetic and internal energy is non trivial for high order

## Proof.

$$\begin{aligned}
 E^{n,*} - E^n &= \sum_i (\overline{\rho_0 e_i^{n,*}} - \overline{\rho_0 e_i^n}) = \sum_i (\overline{\rho_0 \epsilon_i^{n,*}} - \overline{\rho_0 \epsilon_i^n}) + \sum_i \left( \overline{\rho_0 \epsilon_{\text{kin} i + \frac{1}{2}}^{n,*}} - \overline{\rho_0 \epsilon_{\text{kin} i + \frac{1}{2}}^n} \right) \\
 &= -\frac{\Delta t}{\Delta X} \sum_i \sum_{l=1}^s \theta_l \left( \overline{\Pi \delta u_i^{n+\alpha_l}} + \overline{u \delta \Pi_{i+\frac{1}{2}}^{n+\alpha_l}} \right) \\
 &= -\frac{\Delta t}{\Delta X} \sum_i \sum_{l=1}^s \sum_k \sum_{k'} \theta_l \widehat{C}_k d_{k'} \left( \Pi_{i+k}^{n+\alpha_l} u_{i+k+k'+\frac{1}{2}}^{n+\alpha_l} + u_{i+k+\frac{1}{2}}^{n+\alpha_l} \Pi_{i+k+k'+1}^{n+\alpha_l} \right. \\
 &\quad \left. - \Pi_{i+k}^{n+\alpha_l} u_{i+k-k'-\frac{1}{2}}^{n+\alpha_l} - u_{i+k+\frac{1}{2}}^{n+\alpha_l} \Pi_{i+k-k'}^{n+\alpha_l} \right).
 \end{aligned}$$

Making the change of index  $i \leftarrow i + k'$  in the 1st term and  $i \leftarrow i + k' + 1$  in the 2nd term of the RHS:

$$\begin{aligned}
 E^{n,*} - E^n &= -\frac{\Delta t}{\Delta X} \sum_i \sum_{l=1}^s \sum_k \sum_{k'} \theta_l \widehat{C}_k d_{k'} \left( \Pi_{i+k-k'}^{n+\alpha_l} u_{i+k+\frac{1}{2}}^{n+\alpha_l} + u_{i+k-k'-\frac{1}{2}}^{n+\alpha_l} \Pi_{i+k}^{n+\alpha_l} \right. \\
 &\quad \left. - \Pi_{i+k}^{n+\alpha_l} u_{i+k-k'-\frac{1}{2}}^{n+\alpha_l} - u_{i+k+\frac{1}{2}}^{n+\alpha_l} \Pi_{i+k-k'}^{n+\alpha_l} \right) = 0.
 \end{aligned}$$

Lemma 1 gives the conservation of mass, impulsion and total energy as sum of internal and kinetic energies. But because of the non-conservative terms, the computation of internal and kinetic energies is not correct for shocks.

## Proper shock capturing

It is natural to ask when solving system formulated in total energy to be conservative in  $\mathcal{E}^n$  with  $\mathcal{E}^n$  defined as

$$\mathcal{E}^n = \sum_i \overline{\rho_0 \epsilon_i^n} + \sum_i \frac{1}{2} \overline{\rho_0 u_{i+\frac{1}{2}}^{2n}}, \text{ for all } n. \quad (9)$$

We will use the fact  $E^{n,*} = E^n$  and the assumption that for a given  $n$ ,  $\mathcal{E}^n = E^n$ . Setting  $\overline{\rho_0 e_{\text{kin}}^{n+1}}_{i+\frac{1}{2}} = \frac{1}{2} \overline{\rho_0 u_{i+\frac{1}{2}}^{2n+1}}$ , we need to find the formulation of  $\overline{\rho_0 \epsilon_i^{n+1}}$  that truthfully solve the Euler system formulated in total energy.

## Proper shock capturing

$$\begin{aligned} \mathcal{E}^{n+1} - \mathcal{E}^n &= \mathcal{E}^{n+1} - E^{n,*} \\ &= \sum_i \left( \overline{\rho_0 \epsilon_i^{n+1}} - \overline{\rho_0 \epsilon_i^{n,*}} \right) + \left( \frac{1}{2} \overline{\rho_0 u^2}^{n+1}_{i+\frac{1}{2}} - \frac{1}{2} \overline{\rho_0 e_{\text{kin}}}^{n,*}_{i+\frac{1}{2}} \right) \end{aligned}$$

Setting  $\Delta \overline{K}_{i+\frac{1}{2}} = \overline{\rho_0 e_{\text{kin}}}^{n,*}_{i+\frac{1}{2}} - \frac{1}{2} \overline{\rho_0 u^2}^{n+1}_{i+\frac{1}{2}}$ , it yields

$$\begin{aligned} \mathcal{E}^{n+1} - \mathcal{E}^n &= \mathcal{E}^{n+1} - E^{n,*} \\ &= \sum_i \left( \overline{\rho_0 \epsilon_i^{n+1}} - \overline{\rho_0 \epsilon_i^{n,*}} \right) - \Delta \overline{K}_{i+\frac{1}{2}} \\ &= \sum_i \overline{\rho_0 \epsilon_i^{n+1}} - \left( \overline{\rho_0 \epsilon_i^{n,*}} + \Delta \overline{K}_i \right) \end{aligned}$$

which naturally yields the definition of  $\overline{\rho_0 \epsilon_i^{n+1}}$  as  $\overline{\rho_0 \epsilon_i^{n+1}} = \overline{\rho_0 \epsilon_i^{n,*}} + \Delta \overline{K}_i$ . This way, we really solve the lagrangian system formulated in total energy by correcting the internal energy terms. This correction is local.

A high-order accurate synchronization is introduced on point-wise kinetic energies according to (10). For the  $2^{nd}$  order, the synchronization is equivalent to the DeBar fix [DeBar, 1974].

- 1 Compute the difference  $\Delta K$  between point-wise *computed* kinetic energy and point-wise *reconstructed* kinetic energy.
- 2 Distribute  $\Delta K$  on the average values of kinetic energy and internal energy on the stencil.

$$\left\{ \begin{array}{l} \Delta K_{i+\frac{1}{2}} = \rho_0 e_{\text{kin}}^{n,*}_{i+\frac{1}{2}} - \frac{1}{2} \frac{\left( (\rho_0 u)_{i+\frac{1}{2}}^{n+1} \right)^2}{\rho_{i+\frac{1}{2}}^{n+1}} \\ \overline{\rho_0 e_{\text{kin}}^{n+1}}_{i+\frac{1}{2}} = \overline{\rho_0 e_{\text{kin}}^{n,*}}_{i+\frac{1}{2}} - \sum \hat{C}_k \Delta K_{i+k+\frac{1}{2}} \\ \overline{\rho_0 \epsilon_i^{n+1}} = \overline{\rho_0 \epsilon_i^{n,*}} + \sum_k \hat{Q}_{k+\frac{1}{2}} \Delta K_{i+k+\frac{1}{2}} \end{array} \right. \quad (10)$$

## Lemma 2

*The kinetic energy synchronization procedure is conservative in total energy.*

$$\left\{ \begin{array}{l} \phi_{\xi(i)} = \sum Q_{k+\frac{1}{2}} \bar{\phi}_{\xi(i)+k+\frac{1}{2}} \\ \bar{\phi}_{\xi(i)} = \sum_k \widehat{Q}_{k+\frac{1}{2}} \phi_{\xi(i)+k+\frac{1}{2}} \end{array} \right. \quad \text{with } \xi(i) = \begin{cases} i & \text{on primal grid} \\ i + \frac{1}{2} & \text{on dual grid} \end{cases} \quad (11)$$

**Table 3 :** Coefficients for the computation of staggered point-wise values from average values and *vice versa*.

Order	$Q_{\pm\frac{1}{2}}$	$Q_{\pm\frac{3}{2}}$	$Q_{\pm\frac{5}{2}}$	$Q_{\pm\frac{7}{2}}$	$\widehat{Q}_{\pm\frac{1}{2}}$	$\widehat{Q}_{\pm\frac{3}{2}}$	$\widehat{Q}_{\pm\frac{5}{2}}$	$\widehat{Q}_{\pm\frac{7}{2}}$
2 <sup>nd</sup>	$\frac{1}{2}$	0	0	0	$\frac{1}{2}$	0	0	0
3 <sup>rd</sup>	$\frac{7}{12}$	$-\frac{1}{12}$	0	0	$\frac{13}{24}$	$-\frac{1}{24}$	0	0
4 <sup>th</sup> and 5 <sup>th</sup>	$\frac{37}{60}$	$-\frac{2}{15}$	$\frac{1}{60}$	0	$\frac{401}{720}$	$-\frac{31}{480}$	$\frac{11}{1440}$	0
6 <sup>th</sup> and 7 <sup>th</sup>	$\frac{533}{840}$	$-\frac{139}{840}$	$\frac{29}{840}$	$-\frac{1}{280}$	$\frac{68323}{120960}$	$-\frac{353}{4480}$	$\frac{1879}{120960}$	$-\frac{191}{120960}$

## Breaking wave

The Cook-Cabot breaking wave test problem is an initially  $C^\infty$  test case that will transform into a shock. Initial conditions are described in (12) with  $\rho_0 = 10^{-3}$ ,  $p_0 = 10^6$ ,  $\gamma = \frac{5}{3}$  and  $\alpha = 0.1$ . Boundary conditions are periodic and the fluid is supposed to be a perfect gas.

$$\begin{cases} \rho = \rho_0(1 + \alpha \sin(2\pi x)) \\ p = p_0 \frac{\rho}{\rho_0}^\gamma \\ c = c_0 \frac{\rho}{\rho_0}^{(\gamma-1)/2} \\ u = \frac{2}{\gamma-1}(c_0 - c) \end{cases} \quad \text{for } -0.5 \leq x \leq 0.5 \quad (12)$$

"For this set of initial conditions, two of the three characteristics are initially constant, with the third satisfying a Burgers-like equations" ([Cook and Cabot, 2003]). The exact solution until  $t < T_{Shock}$  is the initial profile advected with velocity  $u - c$ .

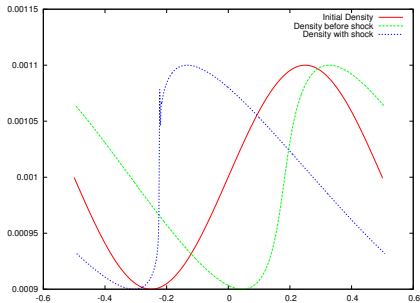
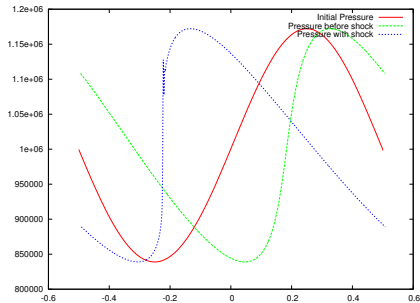


Figure 1 : Pressure and density profiles for the Cook-Cabot breaking wave test-case at  $t = 0$ ,  $t < T_{Shock}$ ,  $t > T_{Shock}$



This time, we are not using a perfect gas, but a gas whose EOS is not convex. The initial conditions satisfies (13).

## Modified breaking wave

$$\left\{ \begin{array}{l} \rho = \rho_0(1 + \alpha \sin(2\pi x)) \\ c(\rho) = \sqrt{\gamma} \rho^{(\gamma-1)/2} + \beta_1 \rho^{\beta_2} \\ p(\rho) = \int c(\rho)^2 d\rho \\ u(\rho) = \int \frac{c(\rho)}{\rho} d\rho \end{array} \right. \quad \text{with} \quad \left\{ \begin{array}{l} \alpha = 0.7 \\ \beta_1 = 0.03 \sqrt{\gamma} \rho_0^{(\gamma-1)/2 - \beta_2} \\ \beta_2 = -4 \\ \rho_0 = 1.4 \\ p_0 = 10^3 \end{array} \right. \quad (13)$$

Once again, the exact solution until  $t < T_{Shock}$  is the initial profile advected with velocity  $u - c$ .

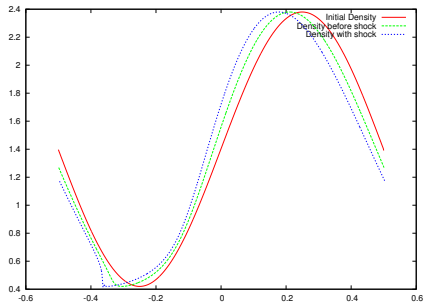
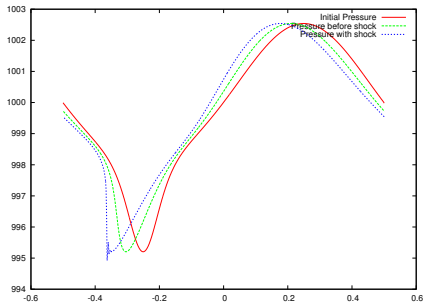


Figure 2 : Pressure and density profiles for the modified Breakingwave test-case at  $t = 0$ ,  $t < T_{Shock}$ ,  $t > T_{Shock}$

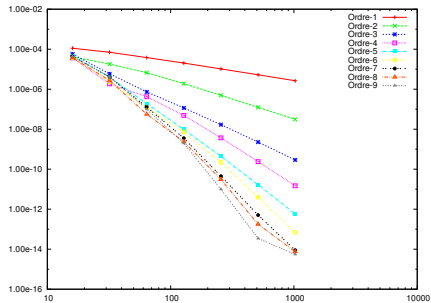
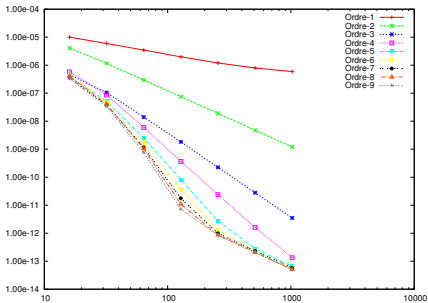
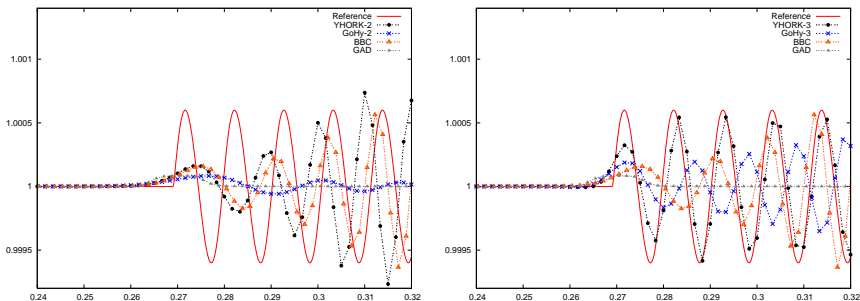
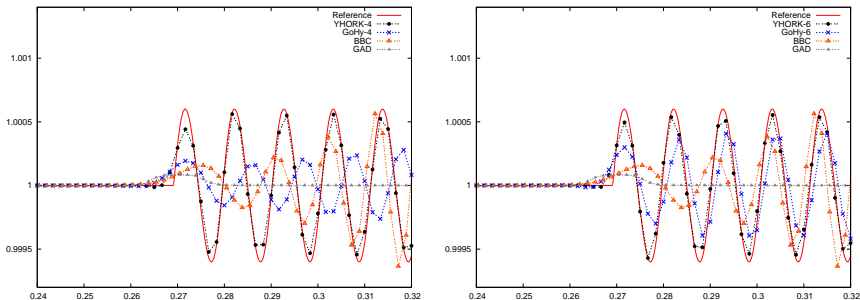


Figure 3 :  $L^1$ -error by number of cells and experimental order of convergence



**Figure 4 :** Acoustic wave with harmonic source - Difference between the GoHy schemes [Duboc et al., 2010] (*cell-centered*), the GAD scheme [Heuzé et al., 2009] ( $2^{nd}$  order *cell-centered*), the BBC scheme ( $2^{nd}$  order *staggered*) and the new *staggered* schemes for order 2 and 3



**Figure 5 :** Acoustic wave with harmonic source - Difference between the GoHy schemes [Duboc et al., 2010] (*cell-centered*), the GAD scheme [Heuzé et al., 2009] ( $2^{nd}$  order *cell-centered*), the BBC scheme ( $2^{nd}$  order *staggered*) and the new *staggered* schemes for order 4 and 6

## 1D-Lagrange-Remap Eulerian schemes

To get back to the original primal and dual grid, we need to perform a projection from the deformed grids to the original grids. From (5) and (6), the primal deformed grid is known.

## Deformed dual grid

After the Lagrange step, the dual deformed grid  $\{x_i^{n+1}\}$  is computed by high-order interpolation of the primal deformed grid  $\{x_{i+\frac{1}{2}}^{n+1}\}$ .

$$x_i = \sum_{k \geq 0} r_k \left( x_{i+k+\frac{1}{2}} + x_{i-k-\frac{1}{2}} \right) \quad (14)$$

with  $r_k$  coefficients in Table 2.

Projection of  $\rho, \rho\epsilon$  on the **primal** grid and of  $\rho, \rho u, \rho e_{\text{kin}}$  on the **dual** one <sup>1</sup>

$$\begin{aligned} \overline{\rho\phi}_j^{n+1} &= \frac{1}{\Delta x} \int_{X_{0j-\frac{1}{2}}}^{X_{0j+\frac{1}{2}}} \rho\phi(x, t^{n+1}) dx \\ &= \frac{1}{\Delta x} \left[ \int_{X_{0j-\frac{1}{2}}}^{x_{j-\frac{1}{2}}} \rho\phi dx + \int_{x_{j-\frac{1}{2}}}^{x_{j+\frac{1}{2}}} \rho\phi dx + \int_{x_{j+\frac{1}{2}}}^{X_{0j+\frac{1}{2}}} \rho\phi dx \right] \end{aligned}$$

Which is equivalent to the flux-form:

$$\overline{\rho\phi}_j^{n+1} = \overline{\rho_0\phi}_j^{n+1} - \left[ \frac{x_{j+\frac{1}{2}} - X_{0j+\frac{1}{2}}}{\Delta x} (\rho\phi)_{j+\frac{1}{2}}^* - \frac{x_{j-\frac{1}{2}} - X_{0j-\frac{1}{2}}}{\Delta x} (\rho\phi)_{j-\frac{1}{2}}^* \right]$$

$(\rho\phi)_{j+\frac{1}{2}}^*$  are computed by *Lagrange* interpolation or *Gauss quadrature* of the desired order.

---

<sup>1</sup>Projection of  $\rho e_{\text{kin}}$  is *unusual* for staggered ones but is the key for proper conservation of total energy.



## Kinetic synchronization procedure

After each remap, the Kinetic synchronization procedure is applied to correct the internal energy.

## Lemma 3

*The projection with kinetic synchronization procedure is conservative in mass, momentum and total energy.*

## Proof.

The projection by itself is conservative in all quantities remap. So mass and momentum are obviously conserved.

As the projection is conservative in internal and kinetic energies, it is conservative for total energy. Besides, kinetic synchronization procedure is also conservative.

So the resulting projection is conservative in mass, momentum and total energy. □

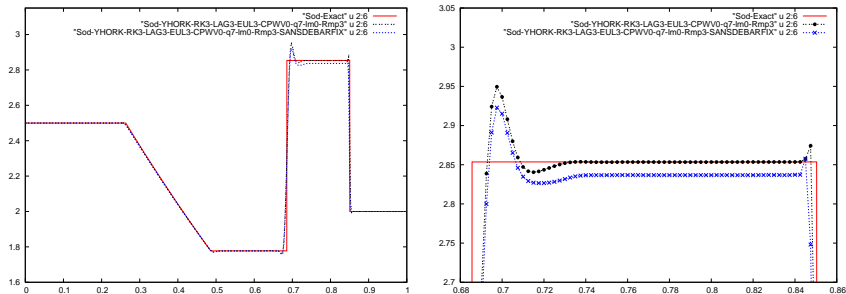


Figure 6 : Respect of Rankine-Hugoniot jump relations (internal energy profile with 400 cells)

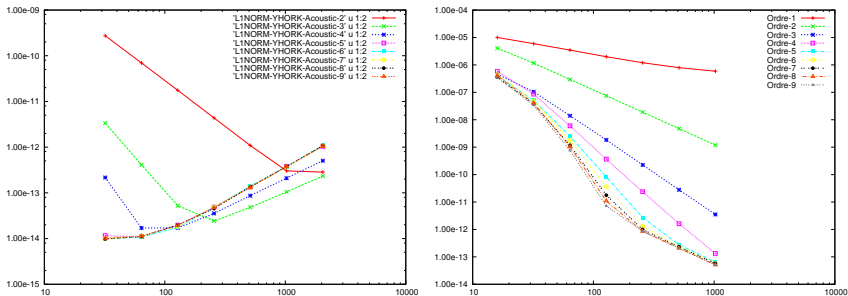
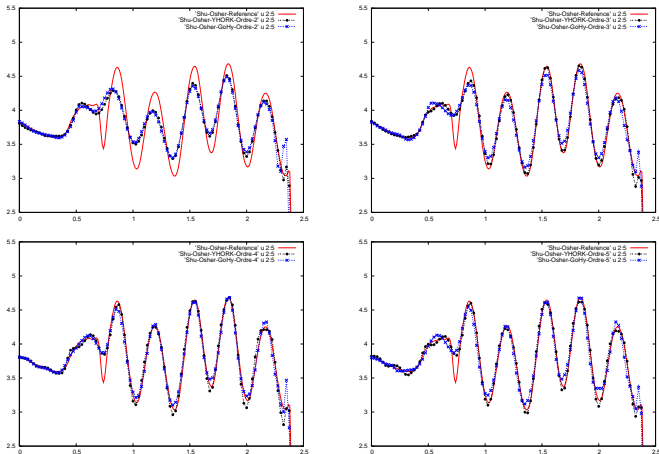
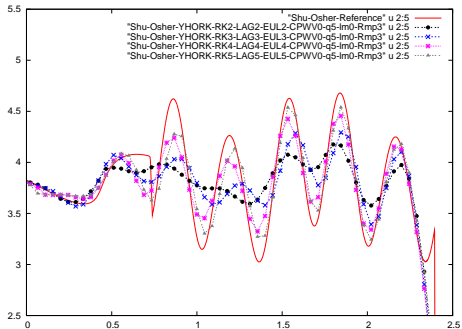
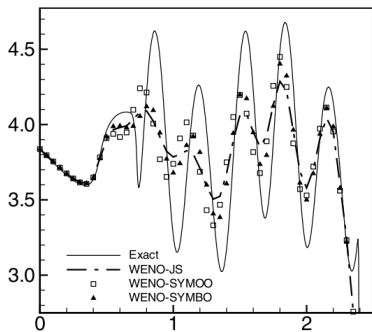


Figure 7 :  $L^1$ -error in both space and time on acoustics (left) and the Cook-Cabot breaking wave test problem (right)



**Figure 8 :** Difference between *staggered* scheme and *cell-centered* GoHy scheme [Duboc et al., 2010] on Shu-Osher test case (nbCell = 400, CFL=0.2, Ordre 2 à 5 ,  $C_\beta = C_\nu = 3.0$ ).



**Figure 9 :** Difference between *staggered* scheme (order 2, 3, 4 et 5) and an direct eulerian code [Martin et al., 2006] WENO5-RK3 on Shu-Osher test case (nbCell = 200, CFL=0.2, Order 2 à 5 ,  $C_\beta = C_\nu = 3.0$ ).

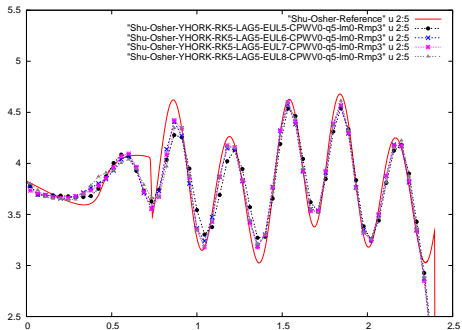
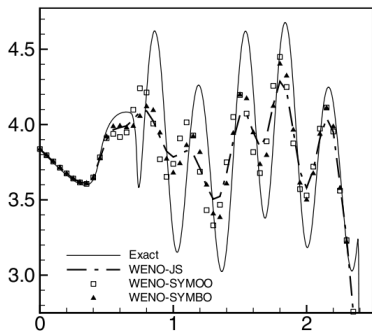


Figure 10 : Difference between *staggered* scheme (order 5, 6, 7 et 8) and an direct eulerian code [Martin et al., 2006] WENO5-RK3 on Shu-Osher test case (nbCell = 200, CFL=0.2, Order 2 à 5 ,  $C_\beta = C_\nu = 3.0$ ).

nD Cartesian grids extension *via*  
high-order accurate directionnal  
splitting

The 1D schemes (5-10) are now to be used with a dimensional splitting method (DSM) on the nD system

## Euler system

$$\begin{cases} \partial_t \rho + \nabla \cdot (\rho \vec{u}) = 0, \\ \partial_t (\rho \vec{\Phi}) + \nabla \cdot (\rho \vec{\Phi} \otimes \vec{u} + \vec{f}) = 0, \end{cases} \quad \text{with} \quad \vec{\Phi} = \begin{pmatrix} \vec{u} \\ e \end{pmatrix} \quad \text{and} \quad \vec{f} = \begin{pmatrix} pI_n \\ p\vec{u}^t \end{pmatrix}. \quad (15)$$

## Arakawa C-type staggering

For the sake of simplicity, we only detail the 2D case. A C-type staggering is retained: variables are indexed  $\phi_{i,j}$  for  $\phi \in \{\rho_0, \rho_0 \tau, \rho_0 \epsilon\}$ ,  $\phi_{i+\frac{1}{2},j}$  for  $\phi \in \{\rho_0, \rho_0 u, \rho_0 e_{\text{kin},u}\}$  and  $\phi_{i,j+\frac{1}{2}}$  for  $\phi \in \{\rho_0, \rho_0 v, \rho_0 e_{\text{kin},v}\}$ .

For a grid with  $N^2 N$  cells, we have to keep in memory  $9N^2$  variables, whereas for MAC-type it is only  $4N^2$  ([Herbin et al., 2013]).



As previous 1D schemes are based on a 1D finite volume formulation, it is mandatory to add a transverse interpolation to deduce 1D-cell-average values from 2D-cell-average ones. The procedure originates from [Duboc et al., 2010] extended here to staggered grids.

## Sweep along $x$ -direction

- 1 Interpolate along the  $y$ -direction to get 1D-cell-average values of the conservative variables according to (7). This way, we only get 1D-cell-average values along the  $x$ -direction.
- 2 Apply the 1D Lagrange scheme with extra equations for  $v$  contributions to momentum and kinetic energy ( $\partial_t \rho_0 v = \partial_t \rho_0 e_{\text{kin},v} = 0$ ). Remap fluxes must be performed on three different grids.
- 3 Reconstruct the 2D fluxes from the 1D Lagrange and remap fluxes according to (7).
- 4 Apply the reconstructed 2D fluxes on 2D-cell-average values.

## Lemma 4

*The resulting 2D Cartesian grid schemes are conservative in mass, momentum and total energy.*

## Proof.

With the C-type staggering of variables, the 2D schemes satisfy Lemmas 1, 2 and 3 direction by direction and so are globally conservative in mass, momentum and total energy for all dimensional splitting. □

## Remarks

The high-order DSM have *negative* time steps which are easily handled as we focus during the remap on the displacement of the Lagrangian grid.

No artificial viscosities/hyperviscosities nor limiters are used in the Lagrange and remap steps. The point-wise kinetic energy synchronization procedure is applied on all cases.

The 2D vortex advection test case is used to assess the accuracy of the schemes. The initial condition is given by (11). Computations are performed on a  $[-10 : 10]^2$  domain till  $t=1$  with  $CFL = 0.9$ ,  $\gamma = 1.4$  and  $\beta = 5$ . The  $L^1$ -errors in both space and time are computed as

$$err_{L^1} = \sum_n \Delta t^n \cdot \Delta x \cdot \Delta y \sum_{i,j} \|\overline{\rho\Phi}_{i,j}^n - \overline{\rho\Phi}_{i,j}^{exact}(t^n)\|_{L^1} \text{ with } \Phi = (1, \vec{u}, \epsilon)^t.$$

## Initial conditions for the Yee Vortex

$$\begin{cases} \rho_0 = \left(1 - \frac{(\gamma-1)\beta^2}{8\gamma\pi^2} e^{1-r^2}\right)^{\frac{1}{\gamma-1}} \\ \vec{u}_0 = \vec{1} + \frac{\beta}{2\pi} e^{\frac{1-r^2}{2}} \cdot (-y, x)^t \\ p_0 = \rho_0^\gamma \end{cases} \quad (16)$$

Order	EOC
2	2.014
3	2.984
4	4.013
5	4.936
6	6.052
7	6.933
8	7.996
9	8.580

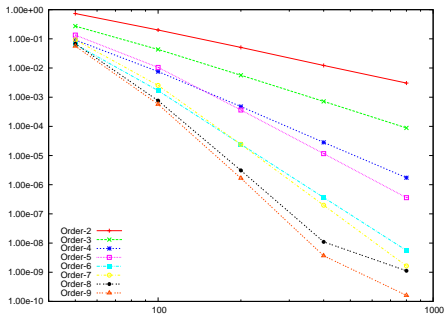


**Figure 11 :** Experimental order of convergence (EOC) on the 2D advected vortex test case from 2nd to 9th-order and  $L^1$ -error in both space and time with respect to the number of cells per direction.

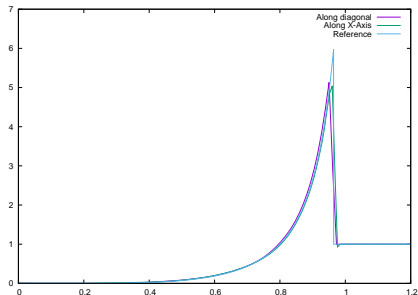
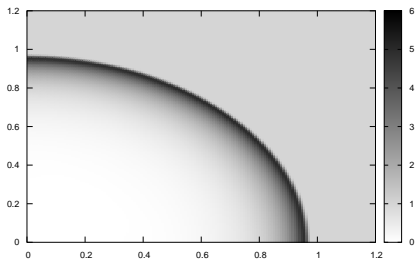
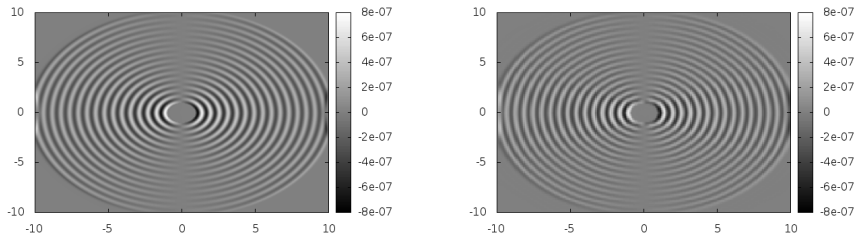


Figure 12 : Sedov blastwave at  $T = 1.0$  for the 3<sup>rd</sup> method with 150 cells in each direction



**Figure 13 :** Difference between 2nd order cell-centered scheme on  $2000 \times 2000$  cells and 4th order staggered scheme on  $200 \times 200$  cells

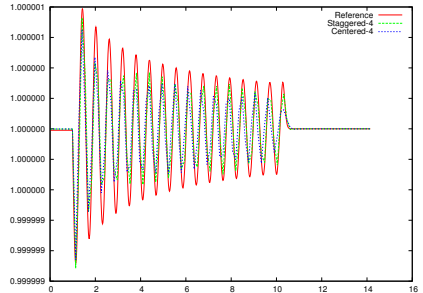
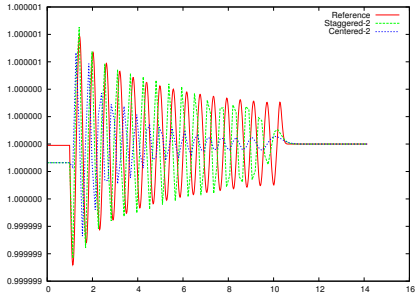
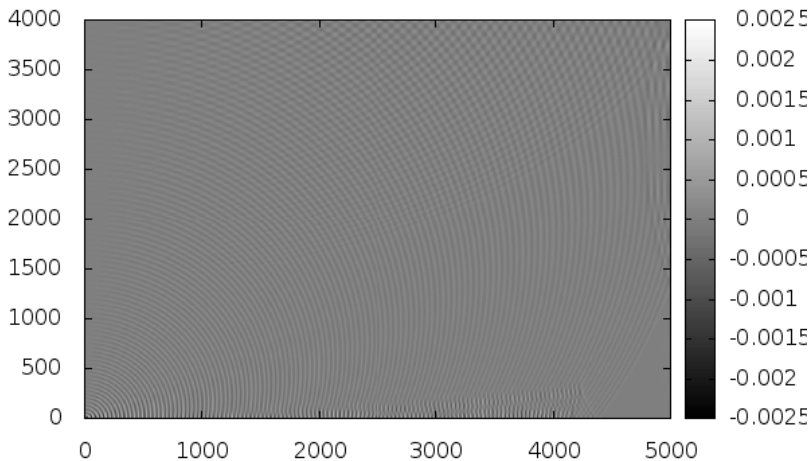
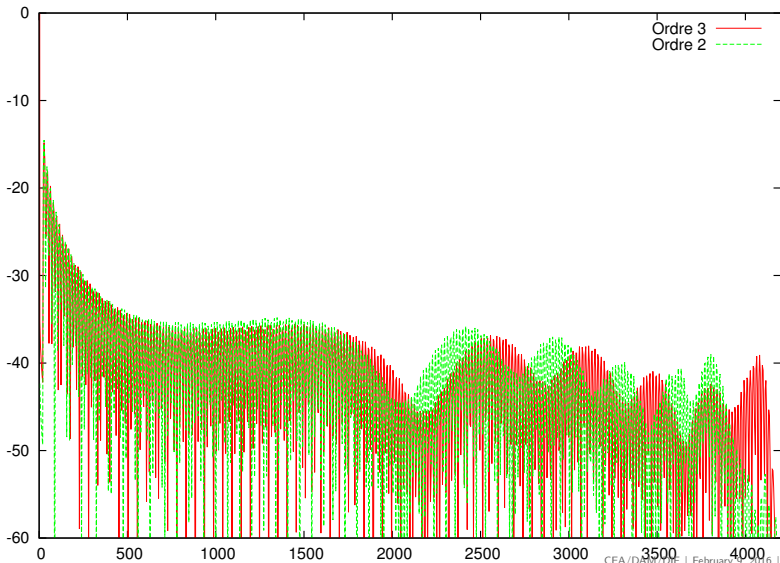


Figure 14 : Diagonal restitution of the acoustic waves for both staggered and cell-centred 2nd and 4th order schemes







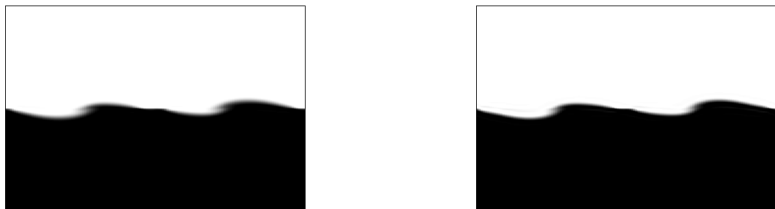


Figure 17 : Vortex-Pairing at  $t = 0.3T$  for the 3<sup>rd</sup> and 7<sup>th</sup> method with 100 cells in each direction

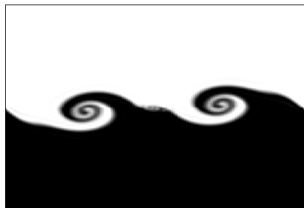
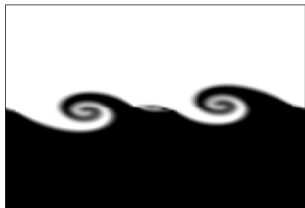


Figure 18 : Vortex-Pairing at  $t = 0.5T$  for the 3<sup>rd</sup> and 7<sup>th</sup> method with 100 cells in each direction

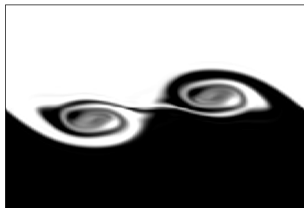
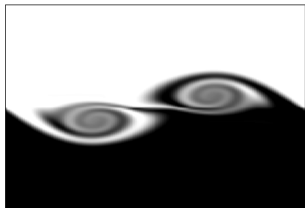


Figure 19 : Vortex-Pairing at  $t = 0.8T$  for the 3<sup>rd</sup> and 7<sup>th</sup> method with 100 cells in each direction

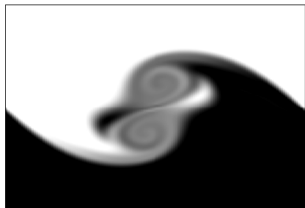


Figure 20 : Vortex-Pairing at  $t = 1T$  for the  $3^{rd}$  and  $7^{th}$  method with 100 cells in each direction

## Conclusions







## Main results

New high-order accurate numerical schemes:

- 1 Formulated in internal and kinetic energies,
- 2 Conservative in mass, momentum and total energy,
- 3 Up to 9<sup>th</sup> order accuracy in 1D due to R–K sequences available [Verner, 2013], and 8<sup>th</sup> order accuracy in nD due to DSM used [Yoshida, 1990],
- 4 C-type staggering of variables which enables better resolution for aeroacoustic waves.

## Perspectives

- Consistency in the sense of Lax to be proven.
- Discrete entropy results.
- Multi-physics extensions (elastic-plastic models, LES/ILES ...)

-  Cockburn, B., Karniadakis, G. E., and Shu, C.-W. (2000).  
*The development of discontinuous Galerkin methods.*  
Springer.
-  Cook, A. W. and Cabot, W. H. (2003).  
A high-wavenumber viscosity for high-resolution numerical methods.  
*J. Comput. Phys.*, 195:594–601.
-  Cook, A. W. and Cabot, W. H. (2005).  
Hyperviscosity for shock-turbulence interactions.  
*J. Comput. Phys.*, 203:379–385.
-  Dakin, G. and Jourden, H. (2016).  
High-order accurate lagrange-remap hydrodynamic schemes on staggered cartesian grids.  
*Comptes Rendus Mathematique.*
-  DeBar, R. B. (1974).  
Fundamentals of the KRAKEN code.  
*Lawrence Livermore Laboratory Report, Technical Report UCIR-760.*
-  Duboc, F., Eaux, C., Jaouen, S., Jourden, H., and Wolff, M. (2010).  
High-order dimensionally split Lagrange-remap schemes for compressible hydrodynamics.





Herbin, R., Latché, J.-C., and Nguyen, T. T. (2013).

Explicit staggered schemes for the compressible euler equations.  
In *ESAIM: Proceedings*, volume 40, pages 83–102. EDP Sciences.



Heuzé, O., Jaouen, S., and Jourden, H. (2009).

Dissipative issue of high-order shock capturing schemes with non-convex equations of state.  
*J. Comput. Physics*, 228:833–860.



Karniadakis, G. and Sherwin, S. (2013).

*Spectral/hp element methods for computational fluid dynamics*.  
Oxford University Press.



Martin, M., Taylor, E., Wu, M., and Weirs, V. (2006).

A bandwidth-optimized WENO scheme for the effective direct numerical simulation of compressible turbulence.  
*J. Comput. Physics*, 220:270–289.



Nagarajan, S., Lele, S. K., and Ferziger, J. H. (2003).

A robust high-order compact method for large eddy simulation.  
*Journal of Computational Physics*, 191(2):392–419.



Nessyahu, H. and Tadmor, E. (1990).

Non-oscillatory central differencing for hyperbolic conservation laws.

*Journal of computational physics*, 87(2):408–463.



Richtmyer, R. D. (1948).

Proposed numerical method for calculation of shocks.

*Los Alamos Report*, 671.



Shu, C.-W. (2003).

High-order finite difference and finite volume weno schemes and discontinuous galerkin methods for cfd.

*International Journal of Computational Fluid Dynamics*, 17(2):107–118.



Shu, C.-W. and Osher, S. (1989).

Efficient Implementation of Essentially Non-oscillatory Shock-capturing Schemes, II.

*J. Comput. Phys.*, 83:32–78.



Sod, G. A. (1978).

A survey of several finite difference methods for systems of nonlinear hyperbolic conservation laws.


*J. Comput. Physics*, 27:1–31.





Sutcliffe, W. G. (1974).


BBC hydrodynamics.


*Lawrence Livermore Laboratory Report, Technical Report UCID-17013*.

 Titarev, V. A. and Toro, E. F. (2002).  
Ader: Arbitrary high order godunov approach.  
*Journal of Scientific Computing*, 17(1-4):609–618.

 Trulio, J. G. and Trigger, K. R. (1961).  
Numerical solution of the one dimensional Lagrangian hydrodynamics equations.  
*Lawrence Radiation Laboratory Report*, Technical Report UCRL-6267.


 Tsoutsanis, P., Kokkinakis, I. W., Könözy, L., Drikakis, D., Williams, R. J., and Youngs, D. L. (2015).  
Comparison of structured-and unstructured-grid, compressible and incompressible methods using the vortex pairing problem.  
*Computer Methods in Applied Mechanics and Engineering*.


 Verner, J. (2013).  
Jim Verner's Refuge for Runge-Kutta Pairs.  
<http://people.math.sfu.ca/jverner/>.

 von Neumann, J. and Richtmyer, R. D. (1950).  
A method for numerical calculation of hydrodynamic shocks.  
*J. Appl. Phys.*, 21:232–237.

 Woodward, P. and Colella, P. (1984).

The numerical simulation of two-dimensional fluid flow with strong shocks.  
*J. Comput. Physics*, 54:115–173.

 Yoshida, H. (1990).  
Construction of higher order symplectic integrators.  
*Phys. Letters A*, 150:262–267.

 Youngs, D. L. (2007).  
"The Lagrangian Remap Method".  
*Implicit Large Eddy Simulation: computing turbulent flow dynamics*,  
Cambridge University Press.